Simulations of the transport and deposition of ^{137}Cs over Europe after the Chernobyl Nuclear Power Plant accident: Influence of varying emission-altitude and model horizontal and vertical resolution

N. Evangeliou[1], Y. Balkanski[1], A. Cozic[1], A. P. Møller[2]

[1]Laboratoire des Sciences du Climat et de l'Environnement (LSCE), CEA-UVSQ –CNRS UMR 8212, Institut Pierre et Simon Laplace, L'Orme des Merisiers, F-91191 Gif sur Yvette Cedex, France

[2]Laboratoire d'Ecologie, Systématique et Evolution, CNRS UMR 8079, Université Paris-Sud, Bâtiment 362, F-91405 Orsay Cedex, France

Correspondence to: Nikolaos Evangeliou (Tel: +33 1 6908-1278, Fax: +33 1 6908-3073, E-mail: Nikolaos.Evangeliou@lsce.ipsl.fr)

Methodology – Parameterisation of deposition (wet and dry), diffusion and convection

The deposition of an atmospheric constituent over a given terrain depends on the local wind speed, the sensible heat, the land-use data (vegetation type, water, soil, etc...), the characteristics of the compound (as e.g. whether it is in gaseous or in particulate form, or both) and on precipitation (cloud physics). Deposition is defined as the amount of the air pollutant (in both forms), which is transferred to the earth's surface by wet and dry removal processes. It is a time dependent process and varies with meteorological conditions and precipitation. In the present study, ^{137}Cs was assumed to be in particulate form (it is treated as a sub-micronic aerosol in accumulation mode following a lognormal distribution), when released from the nuclear power plant, although the particle size was uncertain, ranging between 0.01 and 50 μm, (Valkama and Pollanen, 1996), and as sub-micronic aerosol in wet scavenging.

The LMDz general circulation model distinguishes between stratiform and convective precipitation. The wet scavenging is calculated in INCA for both types of precipitation separately and parameterized as a first-order loss process (Giorgi and Chameides, 1985):

$$\frac{d}{dt}C_g = -\beta C_g \qquad (1)$$

where C_g is the gas phase concentration of the considered species and β the scavenging coefficient (1/s). The scavenging associated with large-scale stratiform precipitation is calculated adopting the falling raindrop approach and calculating the amount of gas removed by the drop falling through each model layer located below the cloud level (Seinfeld and Pandis, 1998). The increase of the aqueous phase concentration C_{aq}^{m} of an irreversibly scavenged gas in a droplet originating from level m and falling through a model layer i (where layer i < layer m) can be estimated by a mass balance between the rate of increase of the mass of species in the droplet and the rate of transfer of species to the drop (Seinfeld and Pandis, 1998):

$$\left[\frac{d}{dt}C_{aq}^{m}\right]_i = \frac{6K_c}{D_p}C_g^i \qquad (2)$$

where C_g^i is the gas phase concentration in layer i encountered by the drop originating from level m, D_p is the rain droplet diameter fixed to a constant value of 3×10^{-3} m in this version of INCA, and K_c the mass transfer coefficient (m s^{-1}). The mass transfer is calculated until equilibrium of the dissolved gas is eventually reached in the falling drop. K_c is calculated with

the relation given by Brasseur et al. (1998). In this relation, we assume a constant value for the drop terminal velocity, we assume that rainout is suppressed at temperatures below 258 ^{o}K.

The scavenging by convective precipitation is calculated as part of the upward convective mass flux on the basis of a modified version of the scheme proposed by Balkanski et al. (1993). On the basis of this formulation and on the basis of equation (1), it can be derived, for the scavenging coefficient associated with convective precipitation,

$$\beta^{cv} = -fF_u \frac{g}{p} \qquad (3)$$

where f is the fraction of soluble gas removed from the gas phase, F_u the upward convective mass flux diagnosed by the GCM (kg m^{-2} s^{-1}), p the pressure and g the gravity constant.

As in the study by Liu et al. (2001), we assume that in the convective column,

$$f = 1 - e^{-a\Delta z} \qquad (4)$$

where Δz (m) is the height in the convective tower calculated from the cloud base. The scavenging efficiency a (m^{-1}) is calculated as the ratio of the rate constant for conversion of cloud water to precipitation (C_{pr}) and the updraft velocity w. On the basis of Mari et al. (2000) and Liu et al. (2001), we adopt C_{pr} = 5×10^{-3} s^{-1}, w = 10 m s^{-1} leading to a = 5×10^{-4} m^{-1}.

The dry deposition of ^{137}Cs was computed using the analogy of surface resistance. The deposition velocity is defined as the inverse of the sum of an aerodynamic resistance and a surface resistance placed in series (Balkanski et al., 1993). They are calculated by the following equation:

$$v_d = \frac{1}{R_a + R_b + R_c} \qquad (5)$$

where R_a, R_b and R_c (s m^{-1}) are the aerodynamical, quasi-laminar, and surface resistances, respectively. R_a and R_b are calculated on the basis of Walcek et al. (1986). The surface resistances are determined for all species included in LMDZORINCA according to their Henry law equilibrium constant and reactivity factor for oxidation of biological substances. The surface resistances are calculated using the vegetation map classification from De Fries and Townshend (1994) interpolated to the model grid and redistributed into the classification

proposed by Wesely (1989). The lower and upper canopy resistances (including stomata, mesophyll, and cuticle resistances) as well as ground resistances are all parameterised according to Wesely (1989). Meteorological variables needed to calculate R_a, R_b and R_c (including temperature, specific humidity, wind speed, precipitation, snow cover, and solar radiation at the surface) are provided by the GCM at each time step. The deposition velocities used in the model for that restricted study area (Europe, 10° W – 80° E, 25° – 75° N) ranged between 0.05 cm s^{-1} over ocean and 0.2 cm s^{-1} over land depending on the period of study. These values are within the range of deposition velocities used in such studies, e.g.0.04 – 0.5 cm s^{-1} (Sehmel, 1980), 0.31 (Slinn and Slinne, 1980), 0.1 cm s^{-1} (Hanna, 1991), 0.05 cm s^{-1} (Maryon et al., 1992) 0.1 – 0.5 cm s^{-1} (Klug et al., 1992) and 0.1 cm s^{-1} (Hwang et al., 2003).

Following Laval et al. (1981), the turbulent eddy diffusivity is computed as:

$$K_z = max\left(l^2 \left\|\frac{\partial \vec{V}}{\partial z}\right\| \sqrt{1 - \frac{R_i}{R_{i_c}}}, K_{min}\right) \qquad (6)$$

where the mixing length l is prescribed as $l = l_0(\frac{p}{p_s})^2$ with $l_0 = 35\,m$, $R_i = ((\frac{g}{\vartheta})(\frac{\partial \vartheta}{\partial z}))/\left\|\frac{\partial \vec{V}}{\partial z}\right\|^2$ is the local Richardson number and $R_{i_c}(= 0.4)$ is a critical Richardson number. Over continents and ice, the value of the minimum diffusivity, $K_{min} = 10^{-7} m^2 s^{-1}$, was tuned in order to get the right strength for the polar inversion (Hourdin et al., 2006). Over oceans, in order to obtain a satisfactory contrast between trade wind cumuli and strato-cumuli on the eastern borders of basins, a diffusion coefficient K_z is first computed with a very small minimum diffusivity $K_{min} = 10^{-10} m^2 s^{-1}$. A second ad-hoc (and generally stronger) diffusivity, $K_z = \xi l^2$ with $\xi = 0.002\ s^{-1}$, is used if the temperature inversion at the boundary layer top is weak (in practice if the maximum value of the vertical gradient of potential temperature, $-\frac{\partial \vartheta}{\partial z}$, is greater than 0.02 K/Pa). The first coefficient is mainly active in the subsidence regions, especially on the East side of oceanic basins. The second one produces smaller (in fact too small) cloud covers in regions of trade wind cumuli. Surface fluxes are computed using parameters (roughness length, albedo, temperature, humidity etc.) adapted to each surface type. For each atmospheric column, vertical diffusion is applied independently for each subsurface, and the resulting tendencies are averaged (Hourdin et al., 2006).

The parameterization of convection in the model is reported by Hourdin et al. (2006). With respect to the Tiedtke's scheme used in previous versions, the Emanuel's scheme

improves the representation of the Hadley–Walker circulation, with a relatively stronger and deeper large-scale ascent over continents, and suppresses the unrealistic patterns of strong rainfall over tropical oceans. Thanks to the regime-sorted framework, originally proposed by Bony et al. (2004) to analyse the cloud radiative forcing and sensitivity, these differences were attributed to intrinsic differences in the vertical distribution of the convective heating and to the lack of self-inhibition by precipitating downdraughts for the Tiedtke's scheme. The combined use of velocity (or z-weighted) potential to characterize the large-scale circulation on the one hand, and regime-sorted approach on the other, appears as a promising framework to work on the validation and improvement of the physical content of atmospheric general circulation models.

References

Balkanski, Y. J., Jacob, D. J., Gardner, G. M., and G.K.K. Turekian: Transport and residence times of tropospheric aerosols inferred from a global three-dimensional simulation of ^{210}Pb. J. Geophys. Res., 98, 20573–20586, 1993.

Brasseur, G. P., Hauglustaine, D. A., Walters, S., Rasch, P. J., Muller, J.-F., Granier, C., and Tie, X. X.: MOZART, a global chemical transport model for ozone and related chemical tracers: 1. Model description, J. Geophys. Res., 103, 28265–28289, 1998.

Bony, S., Dufresne. J,-L,, Le Treut, H., Morcrette, J.-J., Senior, C.: On dynamic and thermodynamic components of cloud changes, Clim. Dyn., 22, 71–86, 2004.

De Fries, R. S., and Townshend, J. R.: NDVI-derived land classification at global scales, Int. J. Remote Sens., 15, 3567– 3586, 1994.

Giorgi, F., and Chameides, W. L.: The rainout parameterization in a photochemical model, J. Geophys. Res., 90, 7872–7880, 1985.

Hanna, S. R., Gifford, F. A., and Yamartino, R. J.: Long range radioactive plume transport simulation Model/Code – Phase I. USNRC Division of Contracts and Property Management, Contract Administration Branch, P-902, Washington, DC 20555. Technical report, pp. 121, 1991.

Hourdin, F., Musat, I., Bony, S., Braconnot, P., Codron, F., Dufresne, J.-L., Fairhead, L., Filiberti, M.-A., Friedlingstein, P., Grandpeix, J.-Y., Krinner, G., LeVan, P., Li, Z.-X., Lott, F.: The LMDZ4 general circulation model: climate performance and sensitivity to parametrized physics with emphasis on tropical convection, Clim Dyn, 27, 787–813, 2006.

Hwang, W.T., Kim, E.H., Suh, K.S., Jeong, H.J., Han, M.H., and Lee, C.W.: Influence of predictive contamination to agricultural products due to dry and wet processes during an accidental release of radionuclides. Ann. Nucl. Energy, 30, 1457–1471, 2003.

Klug, W., Graziani, G., Grippa, G., Pierce, D., and Tassone, C.: Evaluation of long range atmospheric transport models using environmental radioactivity data from the Chernobyl accident, The ATMES Report, Elsevier Applied Science, London and New York, pp. 366, 1992.

Laval, K., Sadourny, R., Serafini, Y.: Land surface processes in a simplified general circulation model, Geophys. Astrophys. Fluid Dyn., 17, 129–150, 1981.

Liu, H., Jacob, D. J., Bey, I., and Yantosca, R. M.: Constraints from ^{210}Pb and ^{7}Be on wet deposition and transport in a global three-dimensional chemical transport model driven by assimilated meteorological fields, J. Geophys. Res. 106, 12109–12128, 2001.

Mari, C., D. J. Jacob, and P. Bechtold: Transport and scavenging of soluble gases in a deep convective cloud, J. Geophys. Res., 105, 22255–22268, 2000.

Maryon, R.H., Smith, F.B., Conwy, B.J., Goddard, D.M.: The UK nuclear accident response model (NAME). Progr. Nucl. Energ., 26 (2), 85–104, 1992.

Sehmel, G.A.: Particle and gas deposition: a review. Atmos. Environ., 14, 983–1011, 1980.

Seinfeld, J. H., and Pandis S. N.: Atmospheric Chemistry and Physics, John Wiley, New York, 1998.

Slinn, S.A., Slinne, W.G.N.: Prediction for particle deposition on natural waters. Atmos. Environ., 14, 1013–1016, 1980.

Valkama, I. and Pollanen, R.: Transport of radioactive materials in convective clouds, In: Proceedings of the 14th International Conference on Nucleation and Atmospheric Aerosols, Helsinki, August 26-30, 1996, (Eds) Kulmala, M. and Wagner, P. E., p. 4, 1996.

Walcek, C. J., Brost, R. A., Chang, J. S, and Wesely, M. L.: SO_2, sulfate and HNO_3 deposition velocities computed using regional landuse and meteorological data, Atmos. Environ., 20, 949– 964, 1986.

Wesely, M. L.: Parametrization of surface resistances to gaseous dry deposition in regional-scale numerical models, Atmos. Environ., 23, 1293–1304, 1989.

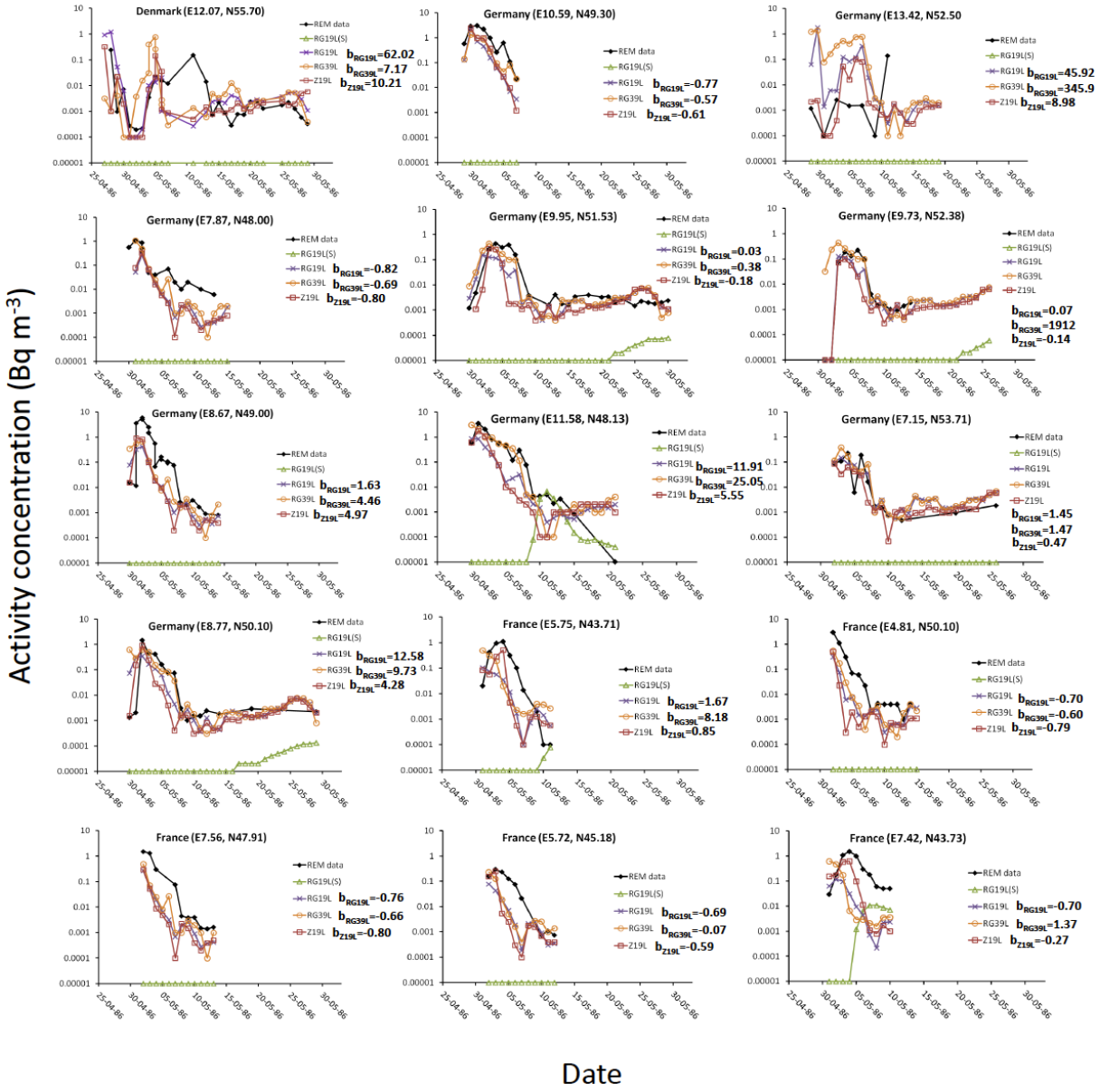

Figure S1. Comparison of the ^{137}Cs surface activity concentrations estimated by all model versions with observations reported in the "REM database" for the Chernobyl accident. The data are available in the website of EU Joint Research Centre in Ispra, Italy. They were examined according to the 3 different directions of the fallout (north, west, south-eastern) on 30th April 1986. The estimated biases are also shown for all the runs (b_RG19L, b_RG39L and b_Z19L) except the one where surface emissions assumed.

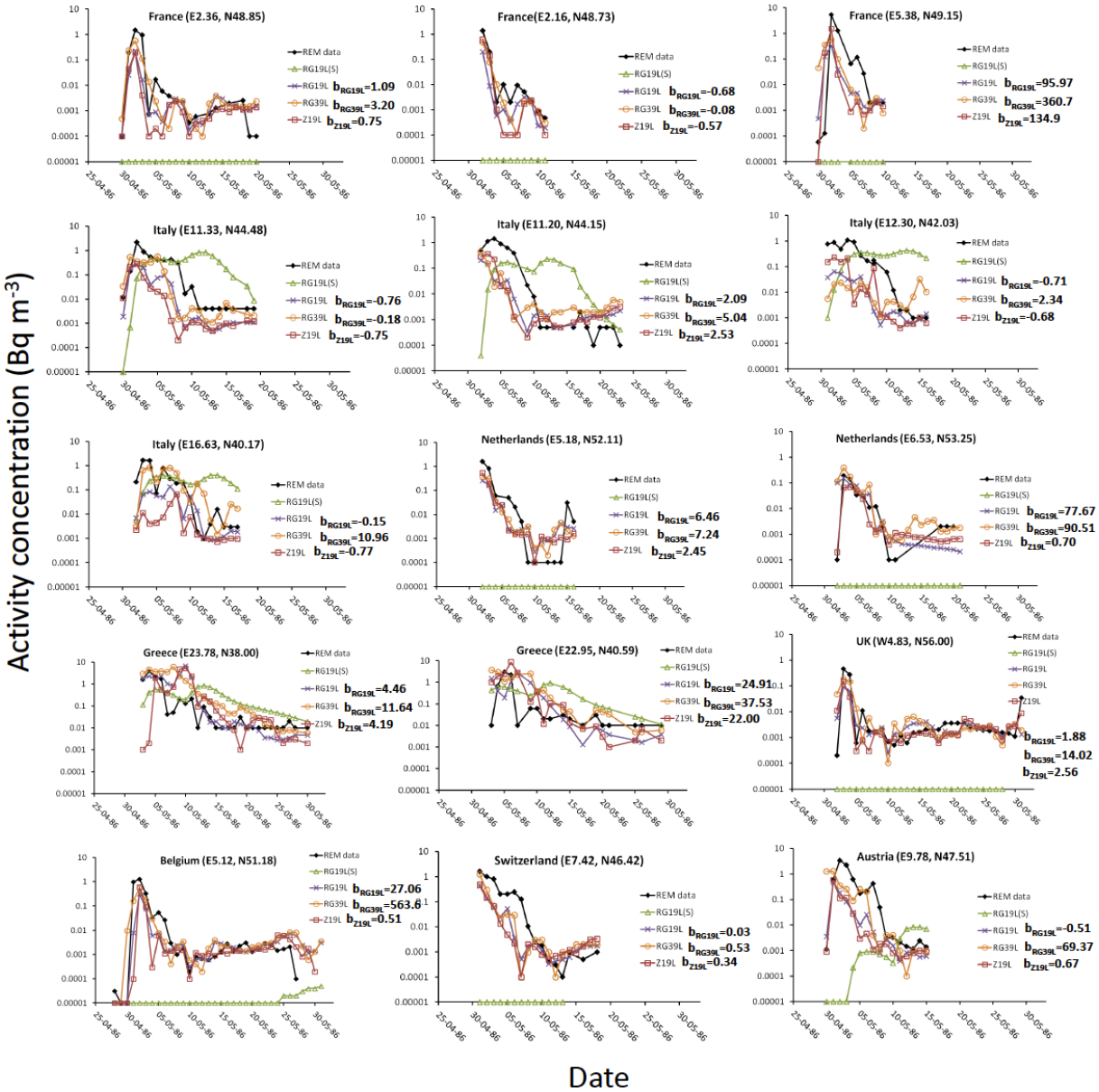

Figure S1. Continued.

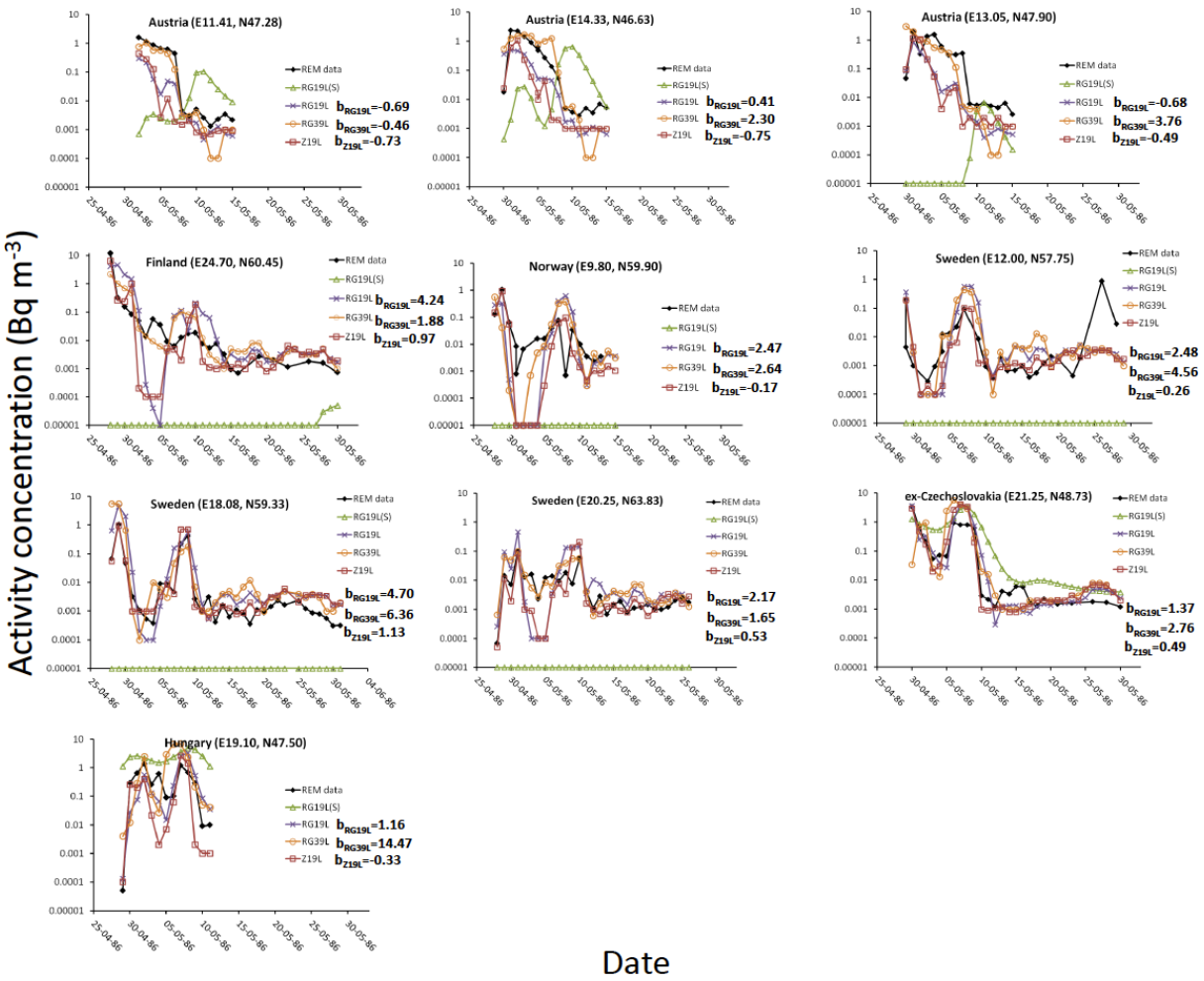

Figure S1. Continued.

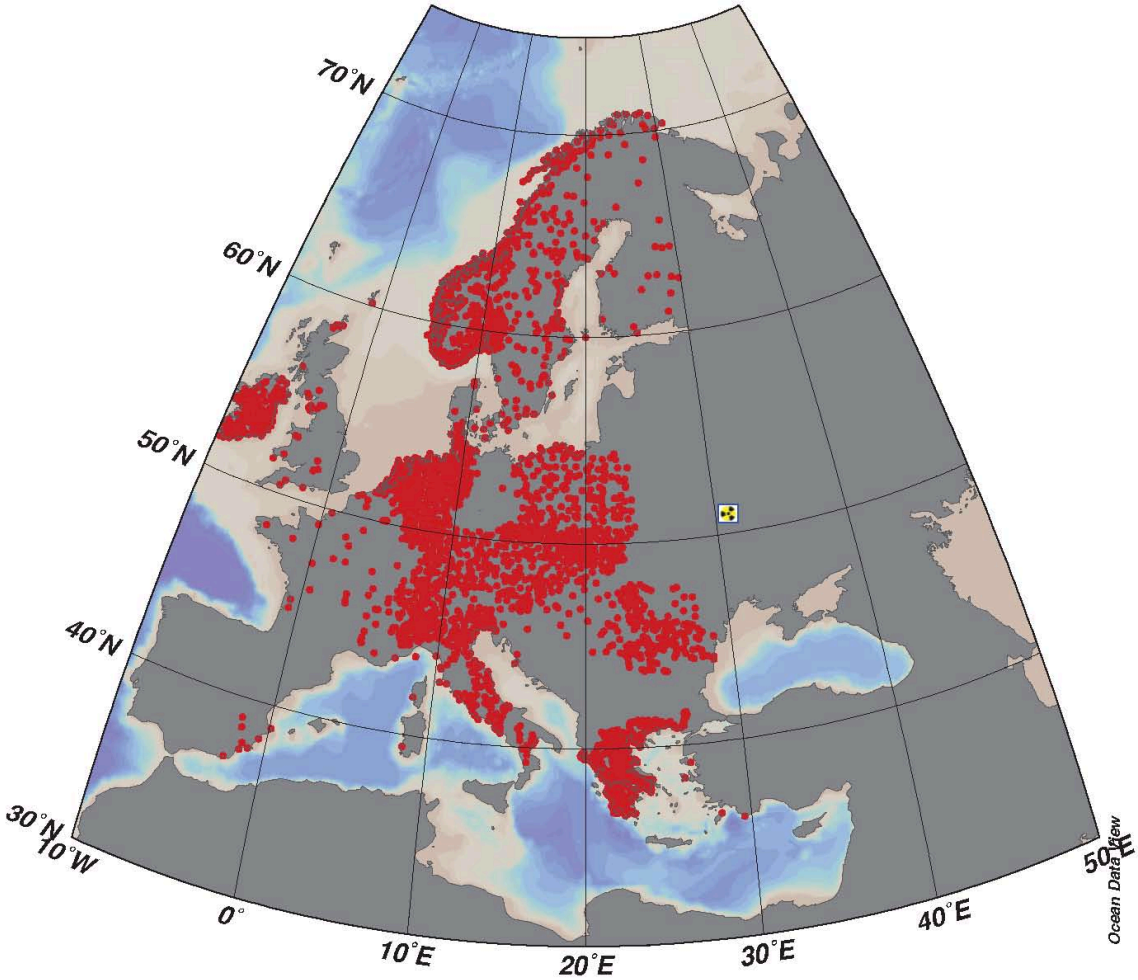

Figure S2. Location of the sampling stations (N = 4266), where measurements of the total deposition of ^{137}Cs after the Chernobyl accident (from the REM database) were carried out. The data were used for the validation of the total deposition of ^{137}Cs resulting from the simulations of the Chernobyl accident using all available versions of the model.

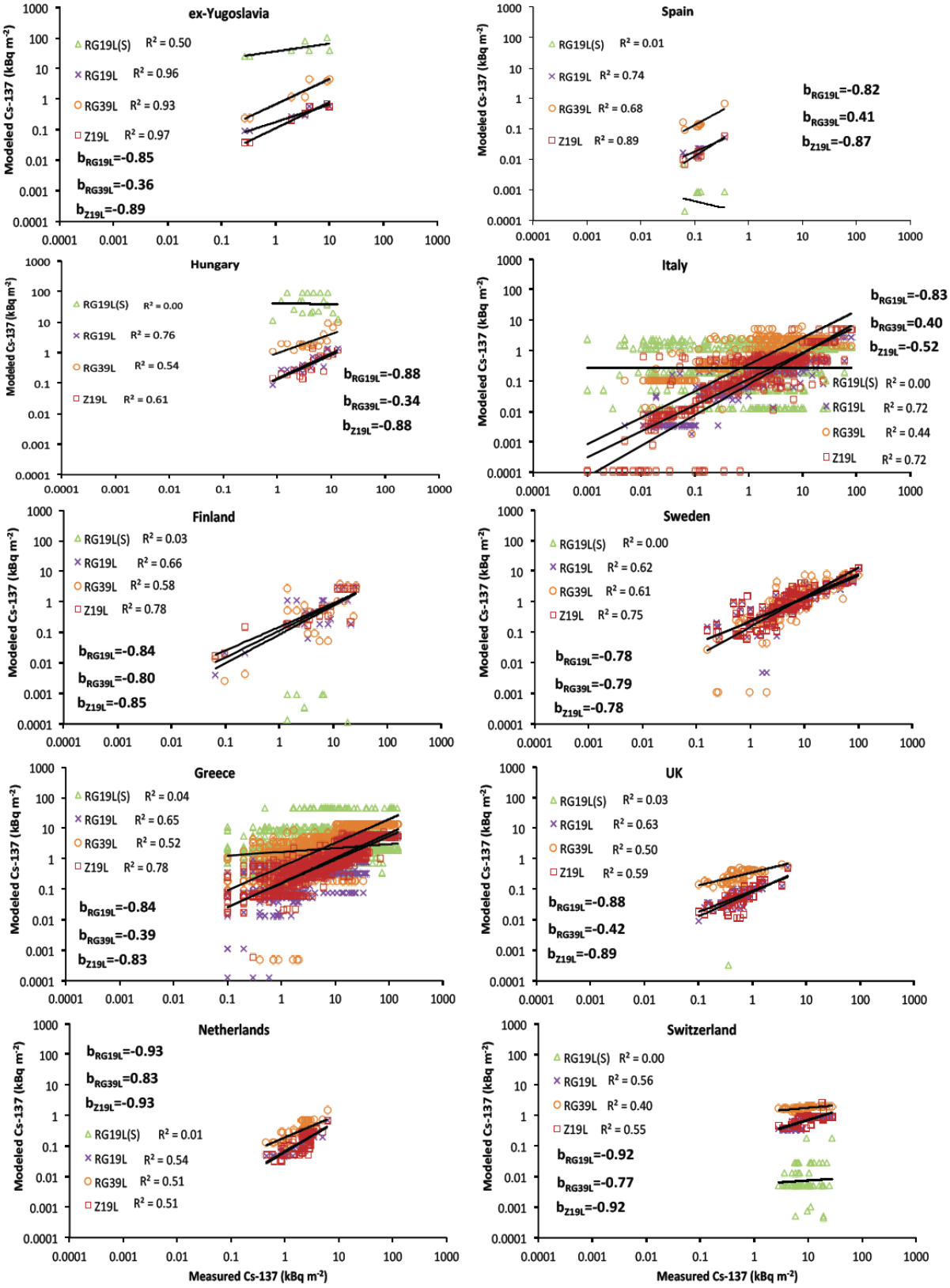

Figure S3. Linear regression scatter plots of the cumulative deposition of ^{137}Cs in 20 European countries from the simulations of all model versions (Modeled Cs-137) and the REM database (Measured Cs-137). The plots are presented in descending order from the best to the worst linear fitting (1 :1). The estimated biases are also shown for all the runs (b_RG19L, b_RG39L and b_Z19L) except for the one where surface emissions assumed.

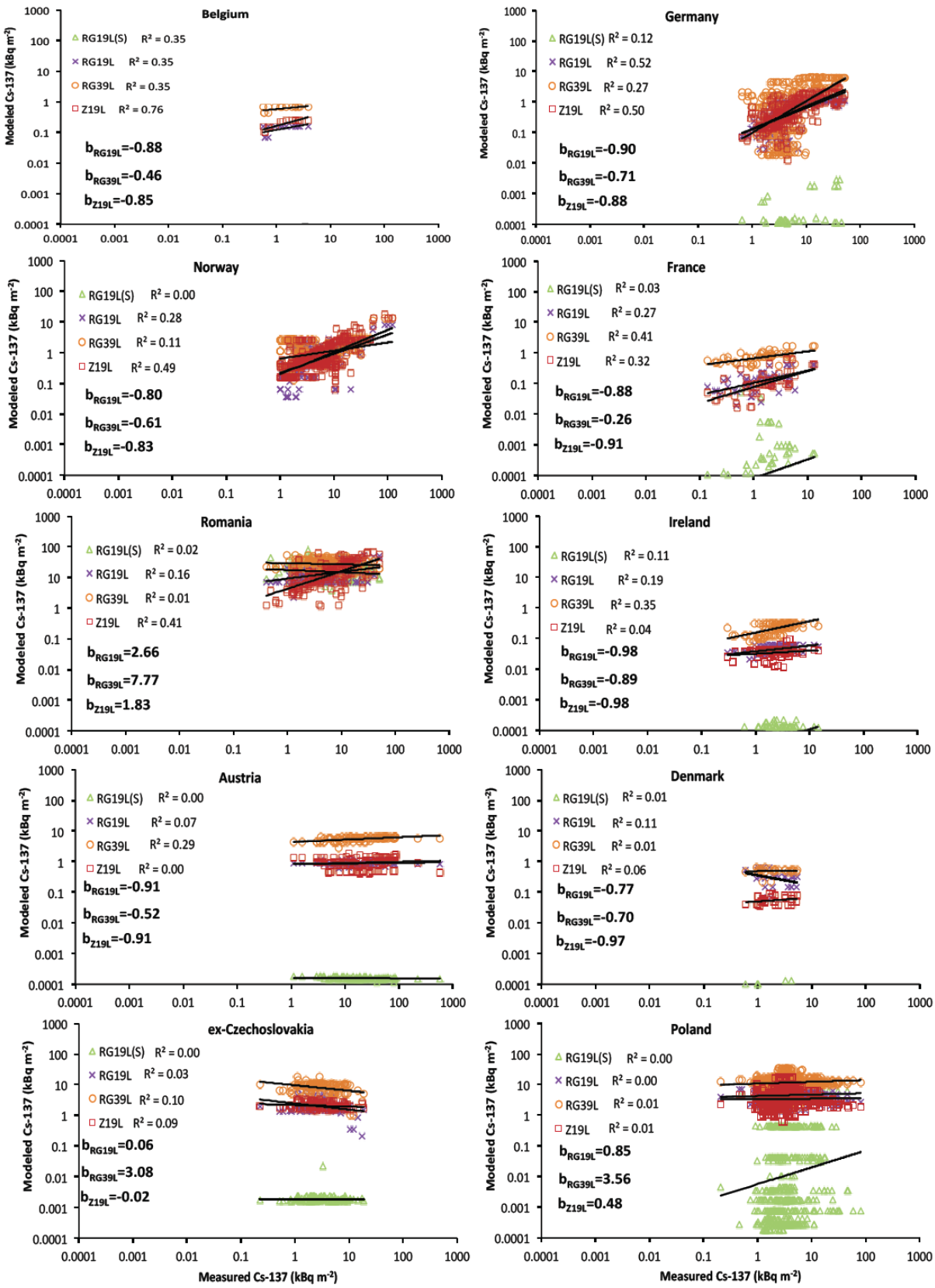

Figure S3. Continued.

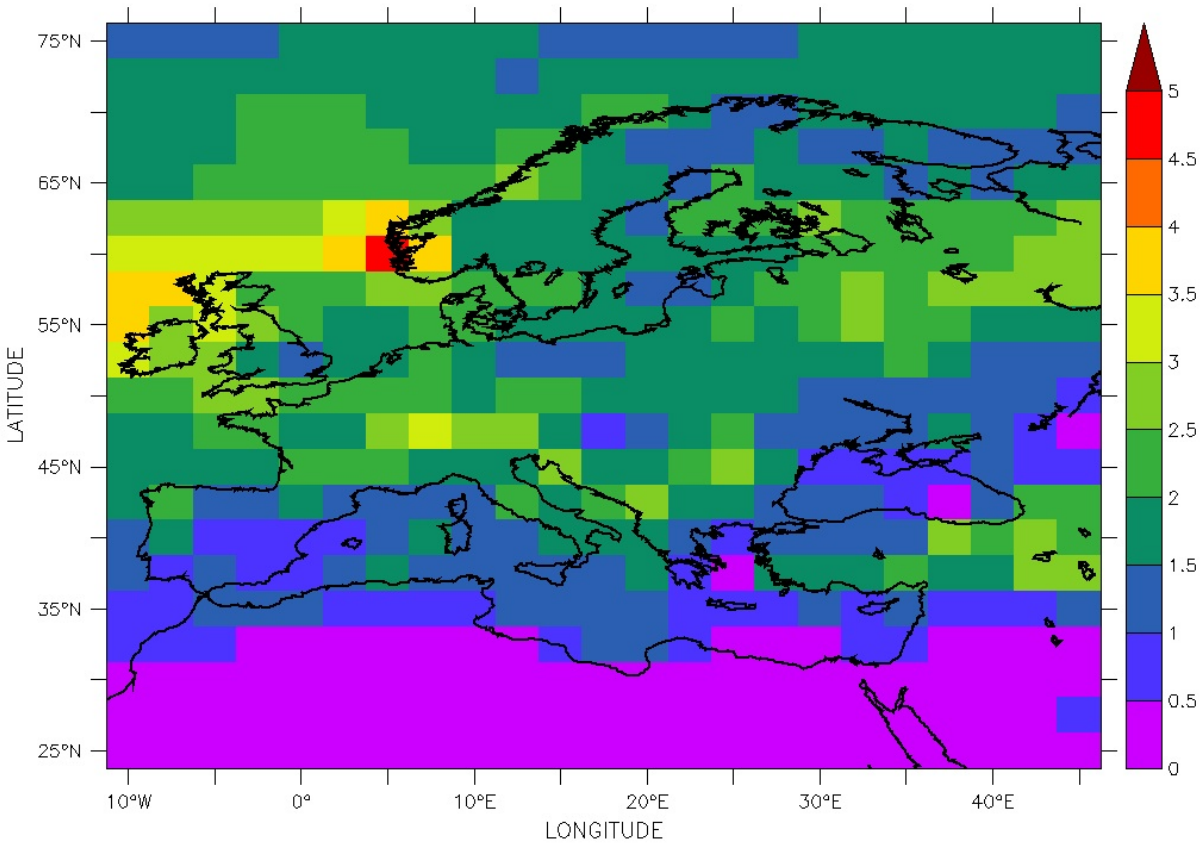

Figure S4. ERA40 (http://data-portal.ecmwf.int/data/d/era40_daily/) (2.5x2.5 degrees) average precipitation (in mm/d) over Europe in 1986.

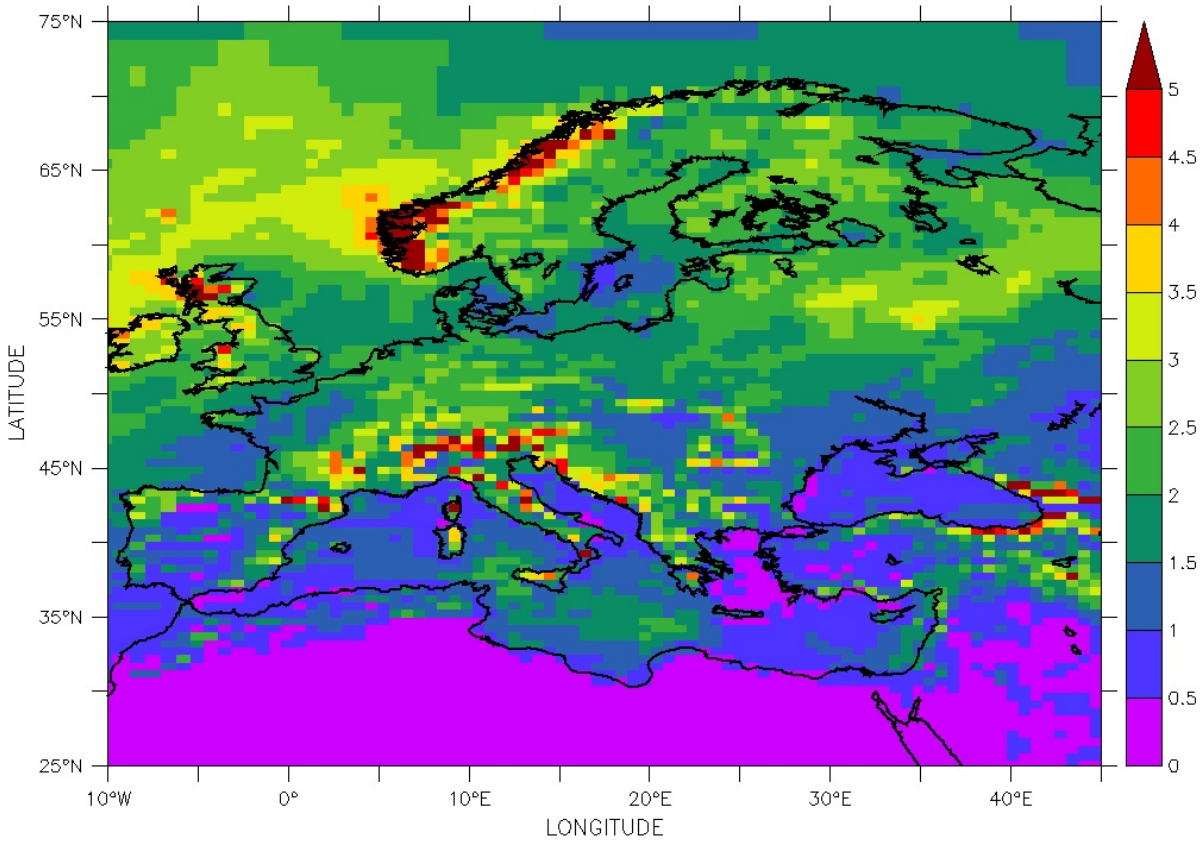

Figure S5. LMDZ (0.66x0.51 degrees) average precipitation (in mm/d) over Europe in 1986.

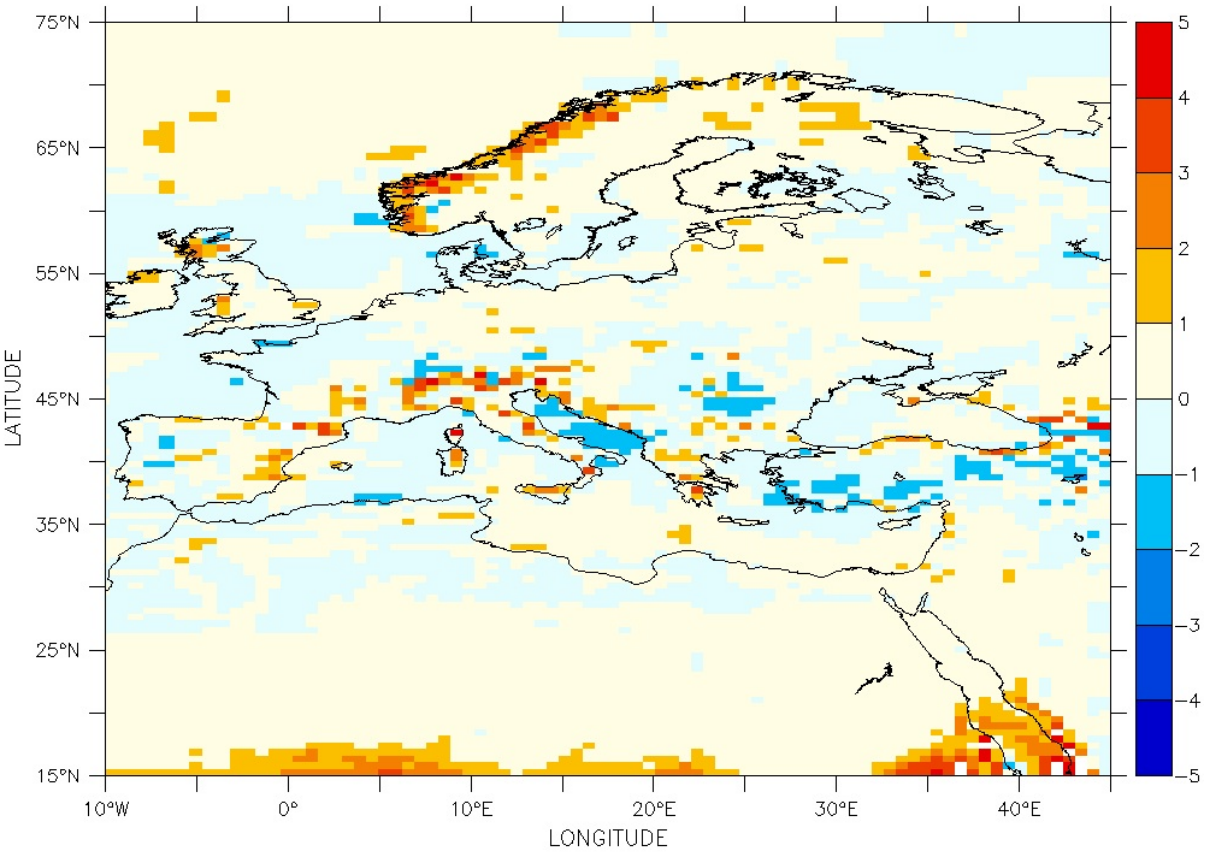

Figure S6. Average difference of precipitation in mm/d between LMDZ model and ERA40 (http://data-portal.ecmwf.int/data/d/era40_daily/) precipitation fields (regridded from 2.5x2.5 degrees to the grid of LMDZ) for the year 1986.

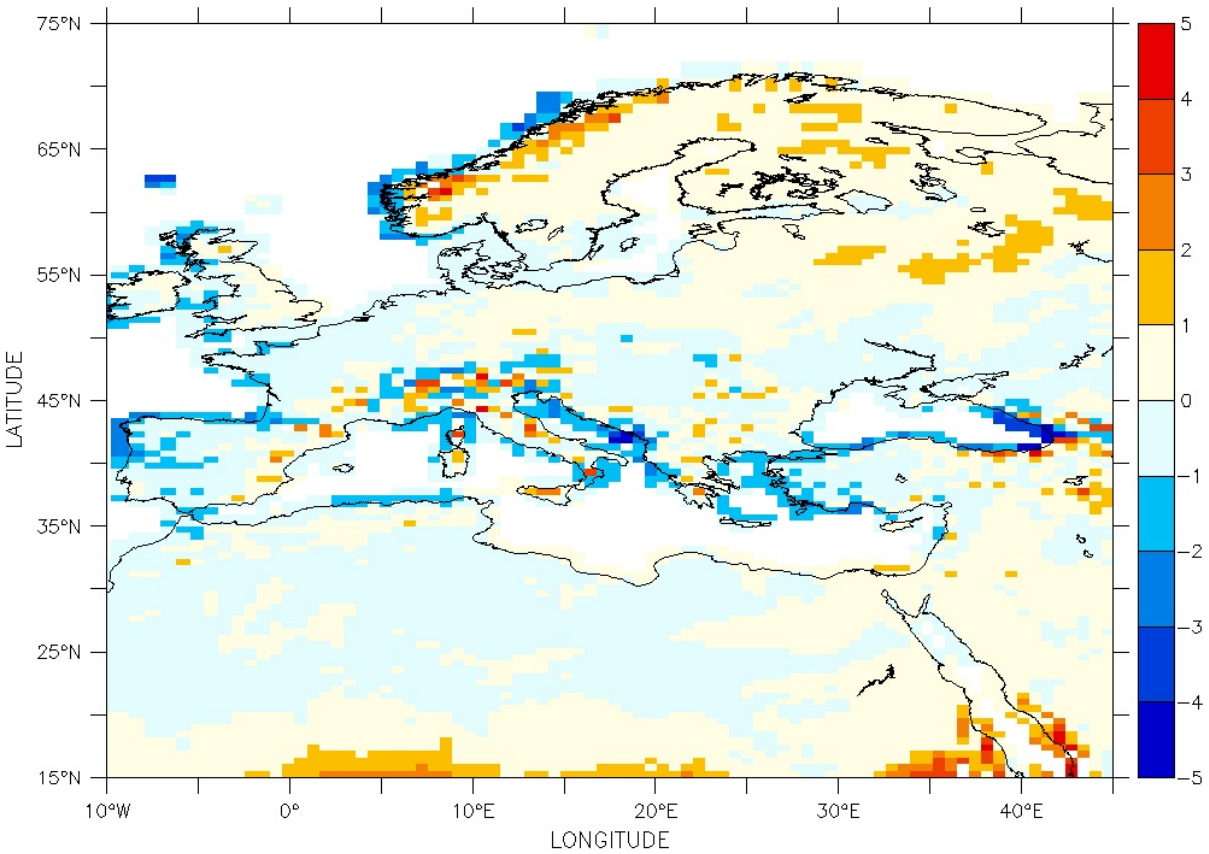

Figure S7. Average difference of precipitation in mm/d between LMDZ (for 1986) and the annual average precipitation fields from the Global Precipitation Climatology Project (GPCC, http://www.esrl.noaa.gov/psd/data/gridded/data.gpcc.html) (in mm/day) for the period 1981-2010 (regridded from 0.5x0.5 degrees to the grid of LMDZ).